# Seasonality and Three-Dimensional Structure of Interdecadal Change in the East Asian Monsoon

RUCONG YU

*State Key Laboratory of Numerical Modeling for Atmospheric Sciences and Geophysical Fluid Dynamics, Institute of Atmospheric Physics, Chinese Academy of Sciences, and State Key Laboratory of Severe Weather, Chinese Academy of Meteorological Sciences, China Meteorological Administration, Beijing, China*

TIANJUN ZHOU

*State Key Laboratory of Numerical Modeling for Atmospheric Sciences and Geophysical Fluid Dynamics, Institute of Atmospheric Physics, Chinese Academy of Sciences, Beijing, China*

(Manuscript received 27 June 2006, in final form 7 February 2007)

ABSTRACT

A significant interdecadal cooling with vivid seasonality and three-dimensional (3D) structure is first revealed in the upper troposphere and lower stratosphere over East Asia. A robust upper-tropospheric cooling appears in March and has two peaks in April and August, but in June, a moderate upper-tropospheric warming interrupts the cooling, while strong cooling occurs in the lower stratosphere. The seasonally dependent upper-tropospheric cooling leads to a clear seasonality of interdecadal changes in the atmospheric general circulation and precipitation against their normal seasonal cycle over East Asia. In March, precipitation over southern China (south of 26°N) has increased in accordance with the strong upper-tropospheric cooling occurring in northeast Asia. In April and May, following the southward extension and intensification of the upper-tropospheric cooling, the normal seasonal march of the monsoon rainband has been interrupted, resulting in a drying band to the south of the Yangtze River valley in late spring. In June, the moderate upper-tropospheric warming and strong lower-stratospheric cooling over northeast Asia has suddenly enhanced the northward migration of the rainband and resulted in an increase of precipitation in the mid–lower reaches of the Yangtze River and farther north. During July and August, the return of upper-tropospheric cooling has weakened the northward progression of southerly monsoon winds, resulting in a mid–lower Yellow River valley (34°–40°N) drought and excessive rain in the Yangtze River valley. The change of surface temperature is well correlated with the change in precipitation, especially in the spring. The surface cooling is generally collocated with excessive rain, while the warming is generally collocated with droughts. Possible causes for the robust interdecadal change are discussed, and stratosphere–troposphere interaction is suggested to play a crucial role in seasonally dependent 3D atmospheric cooling over East Asia.

## 1. Introduction

The East Asian monsoon is an energetic component of the global climate system. During winter, the large Eurasian continent fosters powerful outbreaks of cold air. During summer, the high Tibetan Plateau, acting as an elevated heat source, breeds an imposing subtropical monsoon front extending from the Bay of Bengal and the South China Sea all the way to the North Pacific, bringing abundant rainfall to East Asia and transporting water and energy from the Tropics to the midlatitudes (Tao and Chen 1987). As a result, climate variability in East Asia exhibits many features that challenge our current understanding of climate change. From spring to summer the mechanical forcing of the Tibetan Plateau generates continental middle stratus cloud, which covers a vast area downstream of the Tibetan Plateau. The continental middle-level stratus cloud produces the thickest annual mean cloud optical depth and the strongest net cloud radiative cooling at the top of the atmosphere in the global Tropics and midlatitudes (Klein and Hartmann 1993; Yu et al.

*Corresponding author address:* Rucong Yu, State Key Laboratory of Numerical Modeling for Atmospheric Sciences and Geophysical Fluid Dynamics, Institute of Atmospheric Physics, Chinese Academy of Sciences, Beijing 100029, China.
E-mail: yrc@lasg.iap.ac.cn

DOI: 10.1175/2007JCLI1559.1

2004a). In the past few decades, an interdecadal surface cooling has occurred in some regions of East Asia, in contrast to the common warming trends found elsewhere on the earth (Li et al. 1995; Folland et al. 2001a,b; Hu et al. 2003).

In recent decades, a marked summer precipitation change (often called the "southern-flooding-and-northern-drought" pattern) has been observed in eastern China. Precipitation has increased over the middle and lower reaches of the Yangtze River valley, whereas it has decreased over the middle to lower reaches of the Yellow River valley (Hu 1997; Xu 2001; Hu et al. 2003). These observed interdecadal changes in surface summer rainfall along the middle to lower reaches of the Yangtze River valley and the middle to lower reaches of the Yellow River valley have been regarded as the largest changes in precipitation since A.D. 950 (Xu 2001).

Since an interdecadal change in tropical sea surface temperature (SST) and tropical Pacific convection was observed in the late 1970s (e.g., Nitta and Yamada 1989; Trenberth and Hurrell 1994; Graham et al. 1994; Wang 1995; Zhang et al. 1997), studies on interdecadal changes of the East Asian summer monsoon have usually attributed the driving mechanism to be tropical ocean forcing. For example, the abrupt change of Chinese summer rainfall anomalies occurring in the middle and at the end of the 1970s has been found to be consistent with interdecadal changes in large-scale circulation, namely an intensification and southwestward extension of the western Pacific subtropical high (WPSH) over the subtropical regions of East Asia (Nitta and Hu 1996; Hu 1997). Hu (1997) suggested that the change of SST over the tropical Indian Ocean and tropical western Pacific occurring around 1976–79 partly accounts for the interdecadal change. Gong and Ho (2002) supported this suggestion. According to Chang et al. (2000), above-normal May–June rainfall along the Yangtze River valley followed a warm equatorial eastern Pacific in the preceding winter for both 1951–77 and 1978–96. Wu and Wang (2002) noted that the summer rainfall anomaly along the middle to lower reaches of the Yellow River valley is the result of changes in the ENSO-related East Asian summer circulation anomaly, which is attributed to changes in the location and intensity of anomalous convection over the western North Pacific and India. Ho et al. (2004) found a significant change in summertime typhoon tracks, which are consistent with interdecadal WPSH change. The forcing was also attributed to tropical ocean warming. There have also been studies that have speculated that these interdecadal climate variations might be a result of the increased burning of coal (Xu 2001; Menon et al. 2002).

Recently, Yu et al. (2004b) found a significant interdecadal cooling of upper-tropospheric temperature in East Asia during July and August. The observational evidence raises the possibility that the observed East Asian summer precipitation change might be linked to the tropospheric cooling. Xin et al. (2006) reported a drought-like late spring (21 April–20 May) south of the Yangtze River in recent decades, which could also be explained in terms of upper-tropospheric cooling. Li et al. (2005) demonstrated the relationship between tropospheric cooling and surface cooling downstream of the Tibetan Plateau in March. These recent findings indicate that atmospheric cooling in and above the upper troposphere might have a significant relationship with observed local surface climate change. However, these discussions only pay specific attention to climate change at either the local scale or in a specific season.

The seasonal march of the East Asian summer monsoon displays a stepwise northward and northeastward advance. During the period from early May to mid-May, southern China experiences a premonsoon rainy season. The monsoon rain then extends abruptly from the Indochina Peninsula—the South China Sea—from the Philippines to the Yangtze River valley in early to mid-June and finally penetrates northern China (34°–41°N) in mid-July. The rainy season in northern China generally lasts for one month and ends in the early or middle part of August. From the end of August to early September, the monsoon rain belt rapidly moves back to southern China (Tao and Chen 1987; Ding and Chan 2005). Following the seasonal advance of the East Asian monsoon, the interdecadal change of the East Asian climate should also exhibit some seasonally dependent features. The main motivation of this study is to address the seasonality of interdecadal change in the East Asian monsoon, with particular focus on the interdecadal change of tropospheric cooling, and its relationship with surface climate change. The interdecadal climate change over East Asia is clarified within the context of seasonally dependent three-dimensional (3D) coherent structures.

After describing the data used in this study in section 2, the seasonality and the 3D structure of the East Asian interdecadal cooling is examined in section 3. Section 4 presents the corresponding features of atmospheric circulation change related to the interdecadal cooling, including the changes in tropospheric geopotential height thickness, the East Asian subtropical jet, and low-level winds and pressure. Impacts of the seasonally dependent interdecadal changes in temperature and circulation on surface climate, including the sea-

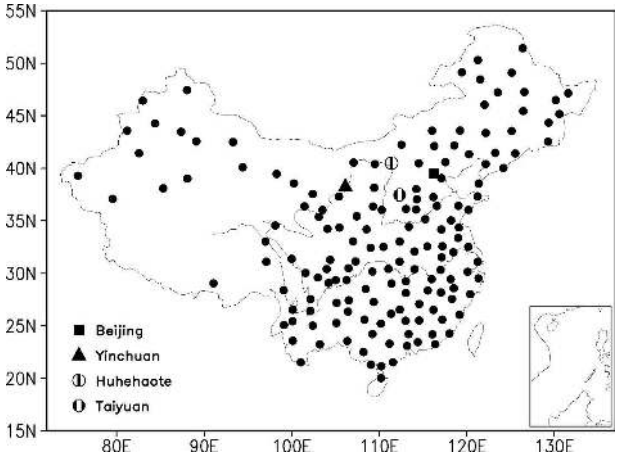


FIG. 1. Locations of rain gauges and four sounding stations. The Yangtze River and the Yellow River are depicted as thin lines.

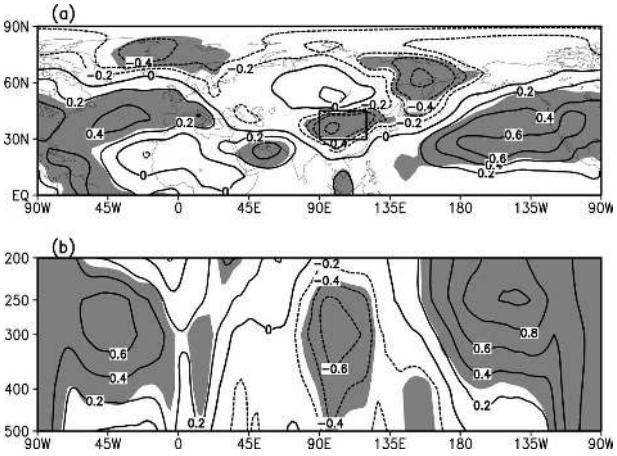


FIG. 2. (a) Long-term change (1980–2001 mean minus 1958–79 mean) of the annual mean temperature averaged vertically in the upper troposphere between 200 and 500 hPa. (b) Longitude–height cross section of annual mean temperature change averaged between 30° and 45°N. Shaded areas are statistically significant at the 5% level according to the Student's *t* test. Units are °C.

sonal migration of the East Asian monsoon rainband, are addressed in section 5. After logically presenting this evidence, we make the point that the southern-flooding-and-northern-drought pattern is part of a much larger picture. This bigger picture exhibits how the 3D structure of East Asian atmospheric cooling contributes to surface climate change. In the final section, we summarize the major points and raise some questions to understand the seasonality of atmospheric cooling.

## 2. Data description

Monthly mean precipitation and surface temperature data at 160 stations in China, and the radiosonde data of four stations located in northern China, were used in this study. This dataset was collected and compiled by the National Meteorological Information Centre of the China Meteorological Administration (CMA). The time period covers 1958–2001. To facilitate analysis, the original observed surface station data were interpolated onto a 1° × 1° grid by averaging the station data with weights proportional to the inverse of the square distance between the grid points and the stations. The four radiosonde stations include Huhehaote (40.82°N, 111.68°E), Beijing (39.80°N, 116.47°E), Yinchuan (38.48°N, 106.22°E), and Taiyuan (37.78°N, 112.55°E). A map showing the location of rain gauges and these four sounding stations is given in Fig. 1.

The atmospheric circulation data were taken from the 40-yr European Centre for Medium-Range Weather Forecasts (ECMWF) Re-Analysis (ERA-40; Uppala et al. 2005). The data used include temperature, geopotential height, and horizontal wind velocity. These variables are on a 2.5° × 2.5° grid covering the period 1958–2001.

## 3. Seasonality and 3D structure of interdecadal cooling over East Asia

Many previous studies have shown that the East Asian climate has experienced decadal shifts in the past decades and the transition point is 1979/80 (Hu 1997; Gong and Ho 2002; Ho et al. 2004; Yu et al. 2004b; Li et al. 2005; Xin et al. 2006). Yu et al. (2004b) presented the discovery of a persistent cooling in the upper troposphere of East Asia in July and August over the last four decades. Here, we inspect this interdecadal change in terms of the annual mean state. Figure 2a shows the long-term change (1980–2001 mean minus 1958–79 mean) of the annual mean temperature averaged vertically in the upper troposphere between 200 and 500 hPa. Figure 2b shows the longitude–height cross section of annual mean temperature change averaged between 30° and 45°N along the meridian. These figures present a vivid contrast between the upper-tropospheric cooling in East Asia and warming elsewhere in the lower–mid latitudes of the Northern Hemisphere. The region of significant cooling covers a large area between 30° and 45°N and from 90° to 120°E, which is located to the northeast of the Tibetan Plateau (hereafter referred to as NETP cooling). The strongest cooling change is near the 300-hPa level in the vertical.

To examine the seasonality of the atmospheric cooling, we present a time–height cross section of monthly

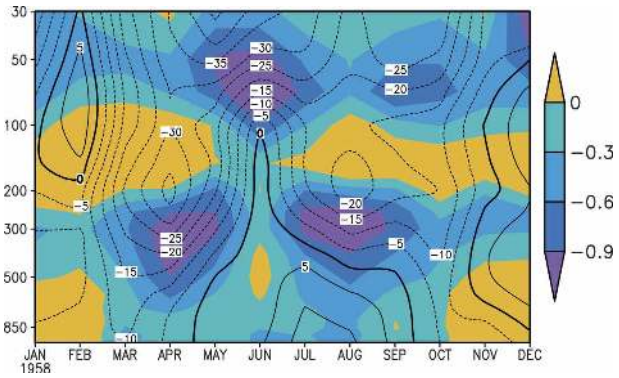


FIG. 3. Time–height cross section of monthly mean air temperature (shading in units of °C) and geopotential height (contours in units of geopotential decameter) changes (1980–2001 mean minus 1958–79 mean) averaged in 30°–45°N, 90°–120°E. The domain selection of 30°–45°N corresponds to the rectangle marked in Fig. 2a and gives prominence to the summer season.

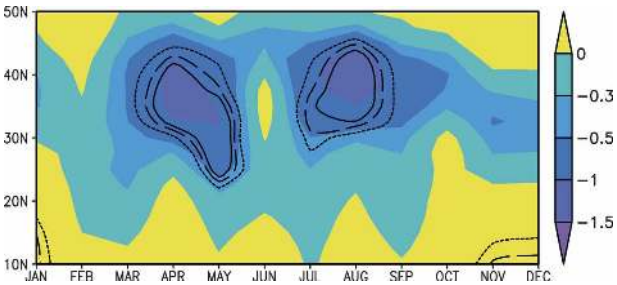


FIG. 4. Time–latitude cross section of 90°–120°E monthly mean temperature changes (1980–2001 mean minus 1958–79 mean) averaged over 500–200 hPa. The short-dashed, long-dashed, and solid lines, respectively, correspond to the thresholds of statistical significance at the 5%, 2%, and 1% levels, according to the Student's *t* test. Units are °C. The domain selection of 90°–120°E corresponds to the rectangle marked in Fig. 2a.

mean air temperature changes averaged over (30°–45°N, 90°–120°E) in Fig. 3. Note that this domain selection corresponds to the cooling rectangle marked in Fig. 2a. Although the annual mean upper-tropospheric cooling is clearly present in East Asia as shown in Fig. 2, the cooling shows a strong seasonal variation. In the troposphere, the strongest cooling vertically occurs around 300 hPa, as mentioned before, and persists throughout the year except in June. There are two peaks in the upper-tropospheric cooling that occur in April and August, respectively. In June, the upper-tropospheric cooling is replaced abruptly by a moderate warming, and the strongest cooling appears in the lower stratosphere. Cooling-induced mass changes result in positive (negative) anomalies of the geopotential height (GPH) beneath (above) the cooling.

As will be shown in Fig. 4, the cooling also has a strong seasonal variation in the meridional direction. To emphasize the condition of the warm seasons, the anomalies were averaged meridionally between 30° and 45°N in Fig. 3. While this is a reasonable choice for summer, it is partial to the north for winter–spring cooling centers, which centered around 20°–45°N. This is the reason why negative rather than positive GPH anomalies are found beneath the maximum cooling region during winter and spring in Fig. 3.

To exhibit the meridional distribution of the cooling change in the upper troposphere, Fig. 4 shows the time–latitude cross sections of 90°–120°E monthly mean temperature changes averaged over 500–200 hPa. The selection of 90°–120°E corresponds to the rectangle marked in Fig. 2a. The two-peak pattern can clearly be seen. The cooling change is restricted meridionally between 20° and 50°N. The springtime cooling center is about 5° south of the summertime cooling center. The spring tropospheric cooling exhibits a southward movement from April to May and suddenly stops in June. From July to August, the tropospheric cooling appears again, except it then has a slightly increased intensity and a more northward location. Hence the interdecadal change of the tropospheric temperature is significantly seasonally dependent and presents a robust 3D coherent structure.

## 4. Seasonality of atmospheric circulation change related to interdecadal cooling

Corresponding to the NETP cooling, large-scale circulations have experienced significant changes over East Asia. The subtropical westerly jet stream, right beneath the tropopause at 200 hPa, is one of the most important circulation systems in East Asia. Its variability reflects major climate variations in this region (Tao and Chen 1987; Zhou and Li 2002). The climatological locations of the jet axis for different months are shown in Fig. 5 by heavy dots. Note that the climatological location of the jet axis is defined as the position of the maximal 100°–120°E averaged zonal wind within 25°–50°N at 200 hPa (Tao and Chen 1987; Zhou and Yu 2005). As a result of the NETP upper-tropospheric interdecadal cooling in late spring and late summer, pressure at the uppermost troposphere decreases, as shown in Fig. 3. This pressure drop increases the poleward pressure gradient force to the south of the cooling region, which in turn enhances the 200-hPa subtropical jet through geostrophic balance between the Coriolis force and pressure gradient force. Hence, the westerly is enhanced south of the 200-hPa jet axis over East Asia, as shown in Fig. 5. The change of the jet stream matches well with that of the cooling in seasonality. Correspond-

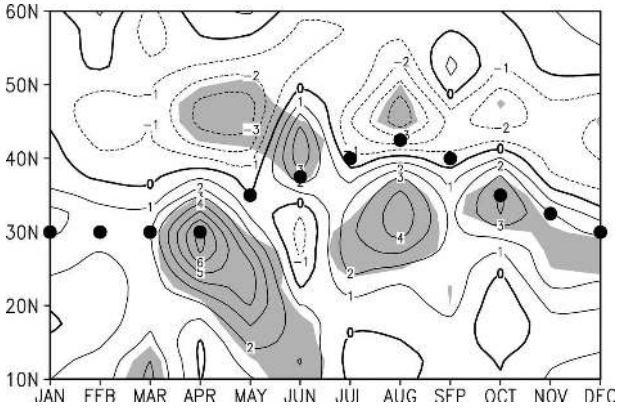


FIG. 5. Time–latitude cross sections of 100°–120°E monthly mean zonal wind changes at 200 hPa (1980–2001 mean minus 1958–79 mean; units: m $s^{-1}$). Heavy dots indicate the climatological locations of the jet axis for different months. Shaded areas are statistically significant at the 5% level according to the Student's *t* test. The domain selection of 100°–120°E corresponds to the climate mean position of the East Asian jet.

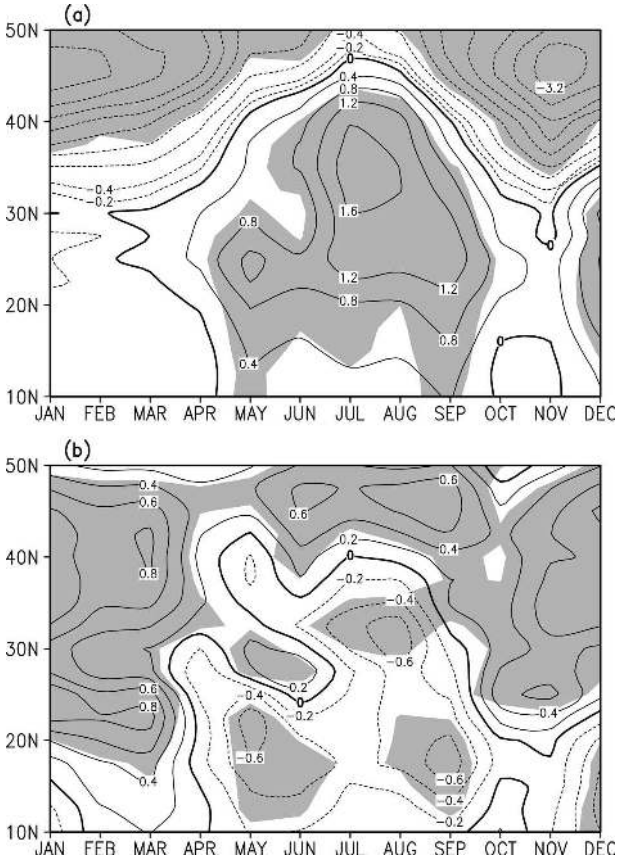


FIG. 6. Time–latitude cross sections of monthly mean changes of (a) 100°–117.5°E averaged sea level pressure (hPa) and (b) 105°–120°E averaged 925–850-hPa meridional wind (m $s^{-1}$). Shaded areas are statistically significant at the 10% level according to the Student's *t* test. The change refers to the difference between 1980–2001 and 1958–79. The selection of 105°–120°E is due to the robust response of the southerly to the east of the anticyclone center.

ing to the peaks of springtime and summertime cooling, the enhancement of the westerly south of the jet axis is most robust in April and August. In addition, between the cooling peaks of April and August, the weak upper-tropospheric warming and the strongest stratospheric cooling in June induce an intensified (weakened) westerly north (south) of the jet stream axis. Observational analyses, for example, Zhou and Yu (2005), have already shown that an intensification of the westerly south of the jet stream over East Asia usually leads to heavier rainfall along the middle and lower reaches of the Yangtze River valley, since an intensified westerly jet stream indicates a stronger high-level zonal divergence, which could favor stronger convections in this area. The westerly change surrounding the jet stream induced by the cooling-related thickness variation should ultimately be manifested in the rainfall field, as will be shown in the following section.

The NETP tropospheric cooling-induced mass change also enhances the lower-tropospheric pressure (below 500 hPa), resulting in an anomalous anticyclone beneath the upper-tropospheric cooling. The center of the anticyclone locates east of the center of the upper cooling. This anticyclone can clearly be seen in the sea level pressure (SLP) change (Fig. 6a), which is a manifestation of the geopotential height change, shown in Fig. 3. Associated with the seasonal variation of the cooling centers shown in Fig. 4, the anomalous anticyclone also experiences robust seasonal migrations, having a spring southern center and a summer northern center. To the east of the anticyclonic center, anomalous northerly winds have increased, which signifies a weakening of the southerly monsoon, as shown in Fig. 6b.

To exhibit the relationship between the temperature changes in the upper troposphere and lower stratosphere and the Asian subtropical jet and meridional flow, correlation coefficients between the regional average temperature anomalies and the zonal (meridional) wind are presented in Table 1. The 200–500-hPa mean temperature anomaly is negatively correlated with the intensity of the 200-hPa zonal wind, and positively correlated with the intensity of the low-layer meridional wind. Since factors affecting the surface wind are more complex than those affecting the upper troposphere, for example, the impact of topography, the correlation coefficients of the upper-tropospheric temperature with the surface meridional wind are not as robust as those with the 200-hPa zonal wind. Nevertheless, they are still statistically significant at the 5% level. Thus, a cooling upper troposphere significantly results in an intensified East Asian upper westerly jet stream and a weakened near-surface southerly monsoon.

TABLE 1. Correlation coefficients of temperature with the westerly and southerly winds. Bold values are statistically significant at the 5% level.

| April $T_{(500–200\ hPa)}$ (30°–45°N, 90°–120°E) | | June $T_{(500–200\ hPa)}$ (30°–45°N, 90°–120°E) | | August $T_{(500–200\ hPa)}$ (30°–45°N, 90°–120°E) | |
|---|---|---|---|---|---|
| $U_{200\ hPa}$ (25°–35°N, 100°–120°E) | $V_{925–700\ hPa}$ (30°–45°N, 90°–120°E) | $U_{200\ hPa}$ (25°–35°N, 100°–120°E) | $V_{925–700\ hPa}$ (30°–45°N, 90°–120°E) | $U_{200\ hPa}$ (25°–35°N, 105°–120°E) | $V_{925–700\ hPa}$ (30°–45°N, 90°–120°E) |
| **−0.76** | **0.45** | **−0.84** | **0.40** | **−0.88** | **0.40** |

According to Fig. 3, June is a transition month, and a moderate warming rather than cooling dominates the upper troposphere. The cooling of the lower stratosphere, however, is intensified in June. The time series of the June 500–200-hPa mean temperature anomalies averaged over the domain (30°–45°N, 90°–120°E) has a significant correlation coefficient of −0.55 with that of the 100–50-hPa mean temperatures, indicating an out-of-phase relationship between the upper-tropospheric and the lower-stratospheric temperature changes. The negative correlation between the 500–200-hPa mean temperature and the 200-hPa jet stream in June, as shown in Table 1, indicates a weakening of the zonal wind between 25° and 35°N. The most prominent feature of Fig. 5 in June is the intensification of the westerly north of the jet stream. In fact, the northern intensification and southern weakening of the zonal wind are coherently linked together and highly correlated with the lower stratospheric cooling. For example, the time series of the zonal wind averaged over the domain (38°–45°N, 100°–120°E) has a significant negative correlation coefficient of −0.51 with the 100–50-hPa mean temperatures averaged over the domain (30°–45°N, 90°–120°E) and −0.65 with that of the zonal wind averaged over the domain (25°–33°N, 100°–120°E), confirming the close connection between the westerly changes south and north of the East Asian jet stream.

## 5. Seasonality of related interdecadal surface climate change

The evidence presented above reveals significant circulation changes associated with the NETP atmospheric cooling. One open question is, what is the corresponding change in the East Asian monsoon rainband?

Based on the 1958–2001 Chinese surface station observations, the seasonality of surface air temperature and precipitation rate changes (1980–2001 minus 1958–79) in eastern China are examined. Figures 7 and 8 show the time–meridional and time–zonal cross sections of changes in precipitation (Figs. 7a, 8a), and surface air temperature (Figs. 7b, 8b) in eastern China, respectively. The seasonal and regional dependences of the changes can be clearly seen. Based on Figs. 7a and 8a, excessive rain mainly occurred in March over southern China and in summer (June, July, and August) along the Yangtze River valley, with a maximum change of around 80% of the climatology; a strong drought-like change occurred in April and May around the Yangtze River valley and in June in southeastern China, with a maximum change of around 50% of the climatology. Compared with the mid–lower Yangtze River valley excessive rain, and the mid–lower Yellow

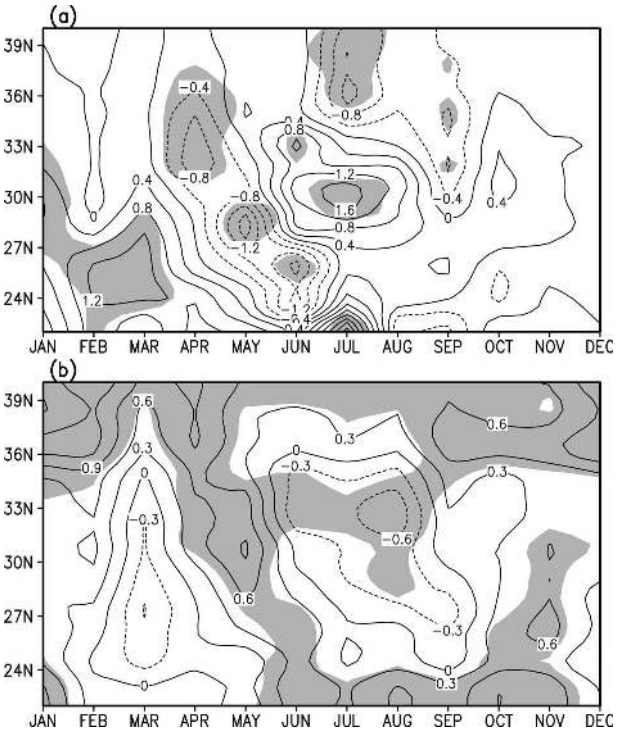


FIG. 7. Time–meridional cross sections of changes (1980–2001 mean minus 1958–79 mean) in (a) precipitation (mm day$^{-1}$), and (b) surface air temperature (°C) in eastern China. The zonal average is taken between 110° and 120°E. Contour intervals are 0.4 for (a) and 0.3 for (b). Shaded areas are statistically significant at the 10% level according to the Student's *t* test.

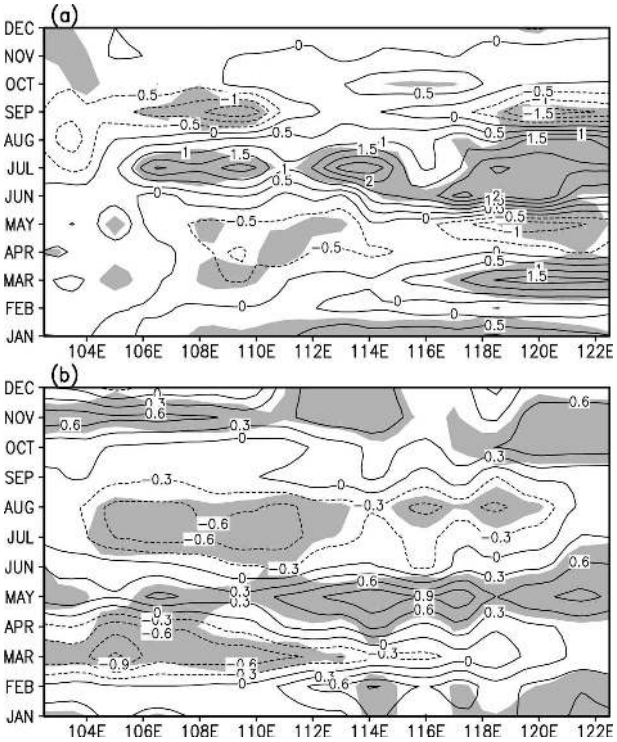


FIG. 8. Time–zonal cross sections of changes (1980–2001 mean minus 1958–79 mean) in (a) precipitation (mm day$^{-1}$), and (b) surface air temperature (°C), along 30°N of eastern China. Contour intervals are 0.5 for (a) and 0.3 for (b). Shaded areas are statistically significant at the 10% level according to the Student's *t* test.

River valley drought in July–August, more rainfall north of 27°N and less rainfall south of it are found in June, appearing as a "southern-drought-and-northern-excessive rain" pattern. From July–August to September, the southern-flooding-northern-drought pattern tends to move southward (Fig. 7a). Of course, the signal for September in Fig. 7a is not as significant as that for July–August; the rainfall change is not as uniform as that for July–August in zonal directions (Fig. 8a), and correspondingly the upper-tropospheric cooling is not very significant in September. In addition, since the changes in precipitation and temperature mainly occurred at specific centers, taking zonal or meridional averages has reduced the significance. Although only areas statistically significant at the 10% level according to the Student's *t* test are shaded in Figs. 7 and 8, further examination of coherent changes in precipitation and temperature centers for specific seasons prove that they are statistically significant at the 5% level (figures not shown), which is consistent with Hu et al. (2003).

Compared with the seasonal movement of the climate mean position of the main rainband, the anomalies of rainfall prior to May indicate a southward shift of the springtime main rain belt. In June, the rainfall center experiences a northward shift. In July, the centers of rainfall anomalies to the west of 112.5°E are generally collocated with the centers of climate mean rain belts, indicating that the rainfall changes are the intensification of the climate mean rainfall centers. The rainfall changes to the east of 112.5°E indicate a southward shift of the rain belt (figure not shown).

Surface cooling mainly occurred in March over southern China and in summer (from June to September) along the Yangtze River valley (Fig. 7b and Fig. 8b). The cooling anomalies are generally collocated with the wetting anomalies, while the warming anomalies are generally collocated with the drought-like anomalies (Nitta and Hu 1996). Changes in increased surface air temperature and decreased precipitation present clear southward movement from April to June.

The observational surface climate changes are closely related to the NETP atmospheric cooling and the associated circulation change, especially in the warm season. From April to August, the changes of the upper-tropospheric temperature and westerly presented dramatic seasonality. As shown in Fig. 9, the temperature changes dominate the changes in the westerly, and comparing with Fig. 7a, the zonal jet change almost determines the change of the surface rain belt. In April, the maximum upper-tropospheric cooling is around 37°N; correspondingly, the westerly is enhanced (weakened) south (north) of 37°N, with the maximum westerly enhancement at around 28°N (Fig. 9a). The changes in precipitation present drought between 28° and 37°N and excessive rain to the south of 28°N, as shown Fig. 7a. In May, the maximum upper-tropospheric cooling moves to 35°N, and the westerly is enhanced (weakened) south (north) of 35°N; the maximum westerly enhancement is around 24°N (figure not shown), which results in the tendency toward increased drought between 25° and 33°N, and excessive rainfall to the south of 25°N (Fig. 7a). In June, the maximum upper-tropospheric warming is around 35°N; correspondingly, the westerly is weakened (enhanced) south (north) of 35°N, with the maximum weakening of the westerly at around 27.5°N (Fig. 9b). The changes in precipitation present flooding between 27.5° and 35°N and drought to the south of 27.5°N (Fig. 7a). In July, the maximum upper-tropospheric cooling is around 37°N; correspondingly, the westerly is enhanced (weakened) south (north) of 37°N, with the maximum westerly enhancement at around 30°N (figure not shown). The precipitation change appears as flooding between 26° and 34°N, and as drought to the north of 34°N (Fig. 7a). In August, the maximum upper-tropospheric cooling moves to 40°N; correspondingly, the westerly is en-

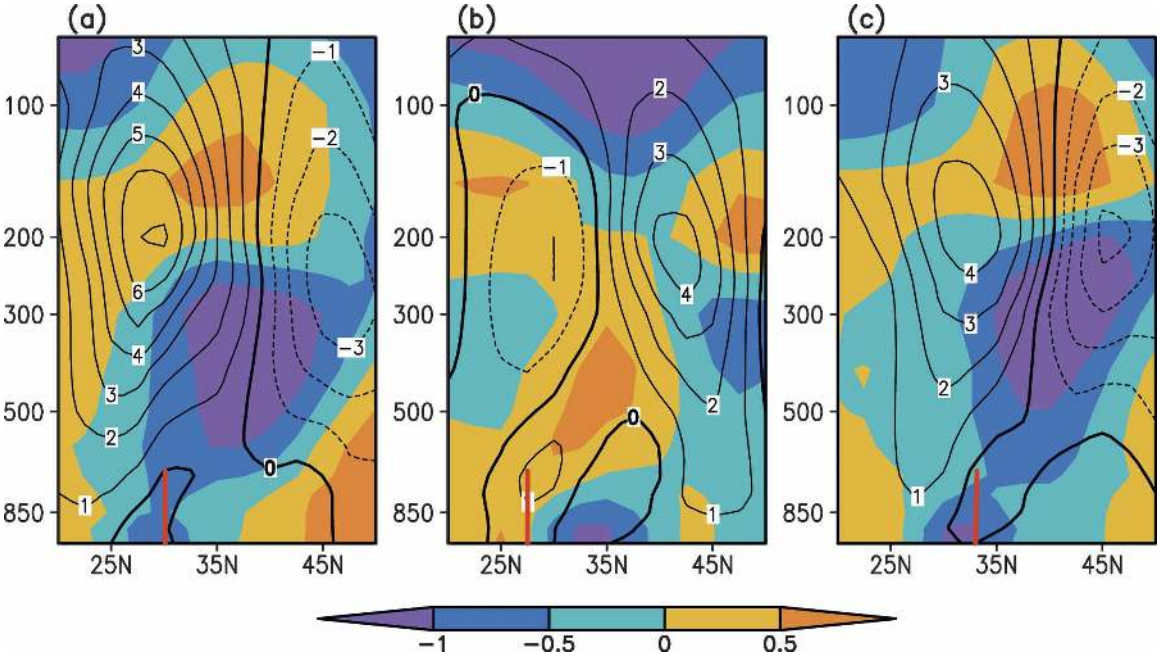


FIG. 9. Latitude–height cross section of (a) April, (b) June, and (c) August mean air temperature (shading in units of °C) and zonal wind (contours in units of m $s^{-1}$) changes (1980–2001 mean minus 1958–79 mean) averaged between 105° and 120°E. The edges between excessive and less rainfall centers of Fig. 7a are marked by red vertical bars.

hanced (weakened) south (north) of 40°N, with the maximum westerly enhancement at around 33°N (Fig. 9c). The changes in precipitation present drought (excessive rain) to the north (south) of 33°N, which is usually called the southern-flooding-northern-drought pattern (Hu 1997; Xu 2001; Hu et al. 2003; Yu et al. 2004b). Thus, the observational surface climate change—in particular the main rainband change—can be explained well in terms of the circulation change associated with interdecadal cooling.

## 6. Summary and discussion

### *a. Summary*

Using station rainfall, surface air temperature, and reanalysis data, the seasonality and 3D structure of the NETP upper-tropospheric interdecadal cooling and the associated surface climate change were analyzed. The major conclusions are summarized below.

1) The upper troposphere of NETP (30°–45°N, 90°–120°E) has experienced a significant interdecadal cooling in recent decades. The cooling has exhibited vivid seasonality and a robust 3D structure. The interdecadal cooling signal becomes robust in March and peaks in April and August.
2) The NETP upper-tropospheric temperature changes correspondingly induced interdecadal changes in atmospheric general circulation, including the East Asian westerly jet, and the lower troposphere southerly. In the upper troposphere, the 200-hPa westerly is enhanced (weakened) to the south of the cooling (warming) center. Beneath the upper-tropospheric cooling, an anomalous anticyclone appears. The southerly located to the east of the anticyclonic center is weakened.
3) The interdecadal changes of Chinese precipitation and surface air temperature are seasonally dependent. Climatologically, a premonsoon rain dominates southern China prior to mid-May; the monsoon rain extends to the Yangtze River valley in early to mid-June and penetrates to the mid–lower Yellow River valley in mid-July, lasting for one month. The abnormal interdecadal changes of the rainfall center indicate a southward shift prior to May, causing the drought south of the Yangtze River valley. From July to August, excessive rainfall dominates the middle and lower reaches of the Yangtze River valley and less rainfall dominates the lower Yellow River valley. The surface cooling is generally collocated with the wetting, while the surface warming is generally collocated with the drought.
4) The seasonality of interdecadal changes in precipitation is linked to that of upper-tropospheric cooling. In March, precipitation over southern China has

increased in accordance with strong upper-tropospheric cooling occurring in northeast Asia. In April and May, following the southward extension and intensification of upper-tropospheric cooling, the westerly is enhanced south of the East Asian subtropical jet; the normal seasonal march of the monsoon rainband has been interrupted, resulting in a drying band in late spring south of the Yangtze River valley. In June, by intensifying the westerly north of the jet stream, the moderate upper-tropospheric warming and strong lower-stratospheric cooling over northeast Asia has enhanced northward migration of the rainband and the precipitation in the mid–lower reaches of the Yangtze River. During July and August, the return of upper-tropospheric cooling has enhanced the westerly to the south of the jet stream and weakened northward progression of the southerly monsoon, resulting in mid–lower Yellow River valley drought and Yangtze River excessive rain.

### *b. Discussion*

The main contribution of this study is to provide a full observational picture of the consistent relationship between upper-tropospheric cooling and surface climate change in East Asia. There are two questions that need to be addressed: 1) How robust is the atmospheric interdecadal cooling given the uncertainties in the ERA-40 data? 2) Why does the atmospheric cooling occur?

To confirm the atmospheric cooling over East Asia, main results based on ERA-40 data were also reexamined by using the National Centers for Environmental Prediction– National Center for Atmospheric Research (NCAR–NCEP) reanalysis data (Kalnay et al. 1996), and the conclusions remain unchanged (figures not shown). In addition, four radiosonde stations over the Chinese domain were selected, including Huhehaote (40.82°N, 111.68°E), Beijing (39.80°N, 116.47°E), Yinchuan (38.48°N, 106.22°E), and Taiyuan (37.78°N, 112.55°E). As shown in Fig. 1, these stations are located exactly beneath the cooling center shown in Fig. 2a. Vertical profiles of the temperature change (1980–2001 mean minus 1958–79 mean) for these four stations are given in Fig. 10. A robust cooling change in the upper troposphere can be clearly observed in all stations of Figs. 10a,b,d, and a warming change can be seen in June (Fig. 10c), proving that the reanalysis data–based results are believable. From the lower to the upper troposphere, the amplitude of the cooling anomaly gradually increases and the strongest cooling occurs at 300 hPa. The seasonal difference of the temperature change is also clear. Besides the warming trend in June, the intensity of the cooling in August is stronger than that in April (Figs. 10b,d).

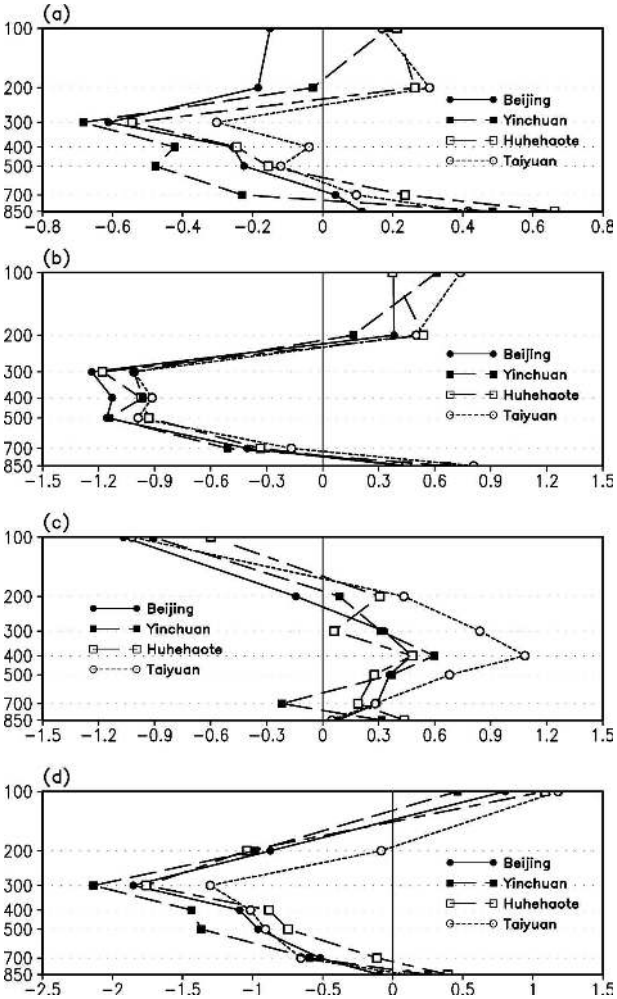


FIG. 10. Vertical profiles of temperature change (1980–2001 mean minus 1958–79 mean) in °C for four stations, including Huhehaote (40.82°N, 111.68°E), Beijing (39.80°N, 116.47°E), Yinchuan (38.48°N, 106.22°E), and Taiyuan (37.78°N, 112.55°E). (a) Annual mean, (b) April, (c) June, and (d) August.

The NETP upper-troposphere and lower-stratosphere temperature changes play important roles in regulating the local circulation changes and thus inducing local climate change. However, causes of the NETP interdecadal cooling remain elusive. Questions involving the physics of the cooling are really challenging our understanding of global climate change and warrant further study to meet a satisfactory answer. As a beginning for this kind of endeavor, we present a discussion on the possible causes for seasonally dependent interdecadal change.

Previous studies have speculated that man-made absorbing aerosols in remote populous industrial regions

alter the regional atmospheric circulation and contribute to regional climate change (Qian and Giorgi 1999; Qian et al. 2001; Xu 2001; Menon et al. 2002). While this argument is plausible for explaining summer surface cooling in central-eastern China, it is not clear whether this can explain why the strongest cooling trend occurs in the upper troposphere and why the cooling trend exhibits significant seasonality. Coupled climate system models with prescribed aerosol forcings have difficulty in reproducing upper-tropospheric cooling (Zhou and Yu 2006). It seems difficult to explain the seasonally dependent interdecadal cooling by the tropical forcing mechanism associated with ENSO (Lau et al. 1998). Yu and Zhou (2004) mentioned that the upper-tropospheric cooling in spring could result from the eastward propagation of a positive North Atlantic Oscillation (NAO) phase–induced cooling signal in North Africa. Yu et al. (2004b) suggested that the upper-tropospheric cooling in July–August could possibly be linked to stratospheric cooling, which may be a part of the integral signal of global warming. Is there any connection between upper-tropospheric cooling changes in spring and July–August? Figures 3 and 4 seem to indicate that no connection exists between the two scenarios, since the moderate tropospheric warming in June broke the tropospheric cooling in spring and late summer. Why does the temperature change present such strong "subseasonal fluctuations"?

Figure 11a presents a time–zonal cross section of temperature change along the subtropical region (30°–40°N) in the troposphere (925–300 hPa), and confirms that the tropospheric cooling in spring results from the eastward propagation of the cooling related to winter NAO in North Africa (Yu and Zhou 2004). The cooling signal reaches Asia in March and intensifies to its maximum in April. Another cross section—the same as in Fig. 11a, except five degrees northward (average in 40°–45°N) and with a focus on the upper troposphere (500–200 hPa)—is shown in Fig. 11b. It is clear that the upper-tropospheric cooling disappears in June over East China, but that there is cooling in the western Pacific. One interesting feature is that, from June to August, the cooling signal retraces its patch westward and reaches East China in July and intensifies in August. Yang et al. (2004) mentioned that the extratropical process related to the NAO is strongly linked to the Asian summer monsoon, which indicates that the summer upper-tropospheric cooling could also be related with NAO. Based on Yu and Zhou (2004), Yang et al. (2004), and Fig. 11, it seems that the interdecadal cooling in spring and late summer is not fully independent and could be linked with NAO behavior. As Ambaum and Hoskins (2002) mentioned that the stratosphere

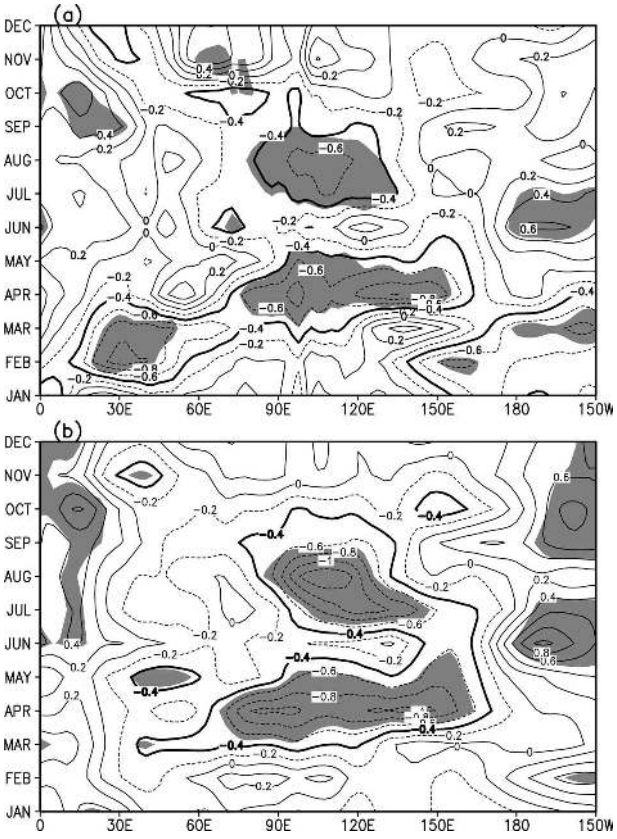


FIG. 11. Time–zonal cross sections of temperature change (1980–2001 mean minus 1958–79 mean) averaged over (a) 925–300 hPa and 30°–40°N, and (b) 500–200 hPa and 40°–45°N. Units are °C. Shaded areas are statistically significant at the 5% level according to the Student's *t* test. The isotherm of –0.4°C is drawn with a thick line.

acts as an integrator of the NAO index, it should not be a conflict that the July–August tropospheric cooling was ever explained by stratosphere–troposphere interaction.

To view a possible connection between the upper-tropospheric and lower-stratospheric cooling anomalies, we present a time–height cross section of monthly mean air temperature changes in (35°–55°N, 115°–135°E) in Fig. 12. There is a cooling signal downward propagation from low stratosphere to upper troposphere from winter to spring, a cooling signal upward from troposphere to stratosphere from April to June, and a cooling signal downward in June and July. Because NAO activity is highly linked to stratospheric behavior, it could not be a conflict that the spring tropospheric cooling over East Asia was explained by NAO impacts (Yu and Zhou 2004) and by downward propagation from low stratosphere to upper troposphere in Fig. 12. Plumb and Semeniuk (2003) suggested that the stratospheric trend could have been

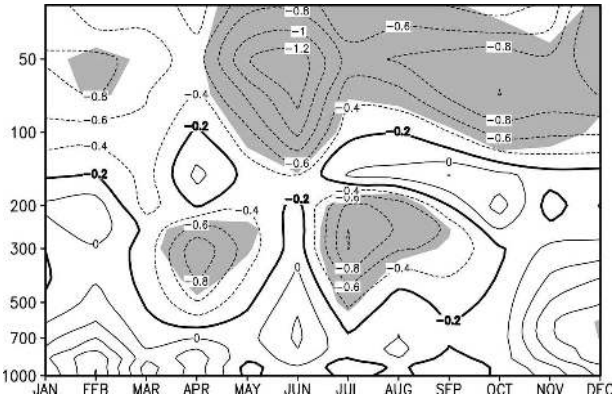


FIG. 12. Time–height cross section of monthly mean air temperature changes averaged in 35°–55°N, 115°–135°E. The change is calculated as the difference between the 1980–2001 mean and 1958–79 mean values. Units are °C. Shaded areas are statistically significant at the 5% level according to the Student's *t* test. The isotherm of –0.2°C is drawn with a thick line.

driven from the troposphere. In July–August, it is confirmed that the tropospheric cooling could be related with downward propagation from the stratosphere (Yu et al. 2004b). Figure 12 indicates that the stratosphere–troposphere interaction could play an important role in the seasonally dependent 3D atmospheric cooling over East Asia.

The above discussion only points out some possible clues to understanding atmospheric cooling and its seasonality, and indicates a physical connection with stratosphere–troposphere interaction. However, for a clear explanation of the causes of Asian air temperature changes, further studies are necessary, including numerical experiments for validation of the suggested mechanism. In addition, the feedback of anomalous rainfall to the upper-air temperature via latent heating change should also be estimated. The most challenging question should be the inserted warming change of the upper troposphere in June against the cooling change in May and July. The abrupt change in June is suggested to relate to the seasonal onset and northward advance of the East Asian monsoon from late May to late June. The decadal change of upper-tropospheric cooling could be hampered by strong seasonal migration. As mentioned in section 5, prior to May, the anomalous rainfall moves reversely with seasonal migration, which could result in a strong rebound of seasonal migration. Strong convection in the sudden advancement of the monsoon rain belt might play a role similar to that in the tropical convective region, enhancing troposphere warming and stratospheric cooling in June.

*Acknowledgments.* This work was jointly supported by the National Natural Science Foundation of China under Grants 40625014, 40675050, and 40221503, and the National Basic Research Program of China (2006CB403603). We appreciated the help of Ms. Xiaoge Xin in producing Fig. 1 and Fig. 10. Comments from three anonymous reviewers were highly appreciated.

## REFERENCES

Ambaum, M. H. P., and B. J. Hoskins, 2002: The NAO troposphere–stratosphere connection. *J. Climate,* **15,** 1969–1978.

Chang, C.-P., Y. Zhang, and T. Li, 2000: Interannual and interdecadal variations of the East Asian summer monsoon and tropical Pacific SSTs. Part I: Roles of the subtropical ridge. *J. Climate,* **13,** 4310–4325.

Ding, Y., and J. C. L. Chan, 2005: The East Asian summer monsoon: An overview. *Meteor. Atmos. Phys.,* **89,** 177–142.

Folland, C. K., and Coauthors, 2001a: Global temperature change and its uncertainties since 1861. *Geophys. Res. Lett.,* **28,** 2621–2624.

——, and Coauthors, 2001b: Observed climate variability and change. *Climate Change 2001: The Scientific Basis,* J. T. Houghton et al., Eds., Cambridge University Press, 99–181.

Gong, D.-Y., and C.-H. Ho, 2002: Shift in the summer rainfall over the Yangtze River valley in the late 1970s. *Geophys. Res. Lett.,* **29,** 1436, doi:10.1029/2001GL014523.

Graham, N. E., T. P. Barnett, R. Wilde, M. Ponater, and S. Schubert, 1994: On the roles of tropical and midlatitude SSTs in forcing interannual to interdecadal variability in the winter Northern Hemisphere circulation. *J. Climate,* **7,** 1416–1441.

Ho, C.-H., J.-J. Baik, J.-H. Kim, D.-Y. Gong, and C.-H. Sui, 2004: Interdecadal changes in summertime typhoon tracks. *J. Climate,* **17,** 1767–1776.

Hu, Z.-Z., 1997: Interdecadal variability of summer climate over East Asia and its association with 500 hPa height and global sea surface temperature. *J. Geophys. Res.,* **102,** 19 403–19 412.

——, S. Yang, and R. Wu, 2003: Long-term climate variations in China and global warming signals. *J. Geophys. Res.,* **108,** 4614, doi:10.1029/2003JD003651.

Kalnay, E., and Coauthors, 1996: The NCEP/NCAR 40-Year Reanalysis Project. *Bull. Amer. Meteor. Soc.,* **77,** 437–471.

Klein, S. A., and D. L. Hartmann, 1993: The seasonal cycle of low stratiform clouds. *J. Climate,* **6,** 1587–1606.

Lau, K.-M., C.-H. Ho, and I.-S. Kang, 1998: Anomalous atmospheric hydrologic processes associated with ENSO: Mechanisms of hydrologic cycle–radiation interaction. *J. Climate,* **11,** 800–815.

Li, J., R. Yu, T. Zhou, and B. Wang, 2005: Why is there an early spring cooling shift downstream of the Tibetan Plateau? *J. Climate,* **18,** 4660–4668.

Li, X., X. Zhou, W. Li, and L. Chen, 1995: The cooling of Sichuan province in recent 40 years and its probable mechanisms. *Acta Meteor. Sin.,* **9,** 57–68.

Menon, S., J. Hansen, L. Nazarenko, and Y. Luo, 2002: Climate effects of black carbon aerosols in China and India. *Science,* **297,** 2250–2253.

Nitta, T., and S. Yamada, 1989: Recent warming of tropical sea surface temperature and its relationship to the Northern Hemisphere circulation. *J. Meteor. Soc. Japan,* **67,** 375–383.

——, and Z.-Z Hu, 1996: Summer climate variability in China and

its association with 500 hPa height and tropical convection. *J. Meteor. Soc. Japan,* **74,** 425–445.

Plumb, R. A., and K. Semeniuk, 2003: Downward migration of extratropical zonal wind anomalies. *J. Geophys. Res.,* **108,** 4223, doi:10.1029/2002JD002773.

Qian, Y., and F. Giorgi, 1999: Interactive coupling of regional climate and sulfate aerosol models over eastern Asia. *J. Geophys. Res.,* **104,** 6477–6500.

——, ——, Y. Huang, W. L. Chameides, and C. Luo, 2001: Regional simulation of anthropogenic sulfur over East Asia and its sensitivity to model parameters. *Tellus,* **53B,** 171–191.

Tao, S., and L. Chen, 1987: A review of recent research on the East Asian summer monsoon in China. *Monsoon Meteorology,* C. P. Chang and T. N. Krishnamurti, Eds., Oxford University Press, 60–92.

Trenberth, K. E., and J. W. Hurrell, 1994: Decadal atmosphere–ocean variations in the Pacific. *Climate Dyn.,* **9,** 303–319.

Uppala, S. M., and Coauthors, 2005: The ERA-40 re-analysis. *Quart. J. Roy. Meteor. Soc.,* **131,** 2961–3012.

Wang, B., 1995: Interdecadal changes in El Niño onset in the last four decades. *J. Climate,* **8,** 267–285.

Wu, R., and B. Wang, 2002: A contrast of the East Asian summer monsoon–ENSO relationship between 1962–77 and 1978–93. *J. Climate,* **15,** 3266–3279.

Xin, X., R. Yu, T. Zhou, and B. Wang, 2006: Drought in late spring of South China in recent decades. *J. Climate,* **19,** 3197–3206.

Xu, Q., 2001: Abrupt change of the mid-summer climate in central east China by the influence of atmospheric pollution. *Atmos. Environ.,* **35,** 5029–5040.

Yang, S., K.-M. Lau, S.-H. Yoo, J. L. Kinter, K. Miyakoda, and C.-H. Ho, 2004: Upstream subtropical signals preceding the Asian summer monsoon circulation. *J. Climate,* **17,** 4213–4229.

Yu, R. C., and T. J. Zhou, 2004: Impacts of winter-NAO on March cooling trends over subtropical Eurasia continent in the recent half century. *Geophys. Res. Lett.,* **31,** L12204, doi:10.1029/2004GL019814.

——, B. Wang, and T. J. Zhou, 2004a: Climate effects of the deep continental stratus clouds generated by the Tibetan Plateau. *J. Climate,* **17,** 2702–2713.

——, ——, and ——, 2004b: Tropospheric cooling and summer monsoon weakening trend over East Asia. *Geophys. Res. Lett.,* **31,** L22212, doi:10.1029/2004GL021270.

Zhang, Y., J. M. Wallace, and D. S. Battisti, 1997: ENSO-like interdecadal variability: 1900–93. *J. Climate,* **10,** 1004–1020.

Zhou, T. J., and Z. X. Li, 2002: Simulation of the East Asian summer monsoon using a variable resolution atmospheric GCM. *Climate Dyn.,* **19,** 167–180.

——, and R. C. Yu, 2005: Atmospheric water vapor transport associated with typical anomalous summer rainfall patterns in China. *J. Geophys. Res.,* **110,** D08104, doi:10.1029/2004JD005413.

——, and ——, 2006: Twentieth-century surface air temperature over China and the globe simulated by coupled climate models. *J. Climate,* **19,** 5843–5858.